Catalytic Subunit Stoichiometry within the Cellulose Synthase Complex[1][W]

Martine Gonneau*, Thierry Desprez, Alain Guillot, Samantha Vernhettes, and Herman Höfte

Institut National de la Recherche Agronomique, Unité Mixte de Recherche 1318, Institut Jean-Pierre Bourgin, Saclay Plant Sciences, F–78000 Versailles, France (M.G., T.D., S.V., H.H.); AgroParisTech, Institut Jean-Pierre Bourgin, F–78000 Versailles, France (M.G., T.D., S.V., H.H.); and Institut National de la Recherche Agronomique, Unité Mixte de Recherche, Microbiologie de l'Alimentation au Service de la Santé, Plateforme d'Analyse Protéomique de Paris Sud-Ouest, Domaine de Vilvert 78352, Jouy en Josas cedex, France (A.G.)

Cellulose synthesis is driven by large plasma membrane-inserted protein complexes, which in plants have 6-fold symmetry. In Arabidopsis (*Arabidopsis thaliana*), functional cellulose synthesis complexes (CSCs) are composed of at least three different cellulose synthase catalytic subunits (CESAs), but the actual ratio of the CESA isoforms within the CSCs remains unresolved. In this work, the stoichiometry of the CESAs in the primary cell wall CSC was determined, after elimination of CESA redundancy in a mutant background, by coimmunoprecipitation and mass spectrometry using label-free quantitative methods. Based on spectral counting, we show that CESA1, CESA3, and CESA6 are present in a 1:1:1 molecular ratio.

Cellulose, the most abundant polymer on earth, is found in plants but also in algae, oomycetes, bacteria, and some animal species. Cellulose consists of 1,4-β-linked glucan chains that assemble into semicrystalline parallel arrays or microfibrils. These microfibrils, with their high tensile strength, have a load-bearing function in plant cell walls. The pattern of association of glucan chains, and hence the size and shape of the microfibrils, depend on the organization of the plasma membrane-embedded cellulose synthase complex (CSC; Tsekos, 1999; Brown and Saxena, 2007). For instance, many bacteria and various algae form linear arrays of multiple cellulose synthase catalytic subunits (CESAs), which synthesize ribbon-shaped microfibrils. Charophytes and land plants, instead, have hexameric CSCs, also referred to as rosettes, which produce elementary microfibrils with a cross section of around 3 nm and which can form higher order aggregates, depending on the cell types and the growth stage (Ding and Himmel, 2006; Harris et al., 2010). Recently, the crystal structure of the cellulose synthase subunit A (BcsA) of *Rhodobacter sphaeroides* in complex with the accessory protein BcsB was solved (Morgan et al., 2013). The structure shows that each CESA subunit has a single catalytic site that synthesizes the 180° alternating glycosidic bonds of the glucan chain. Plant CESAs are encoded by a multigene family; for instance, Arabidopsis (*Arabidopsis thaliana*) has 10 CESA isoforms. The catalytic domain of plant CESAs is homologous to that of the bacterial CESAs (Pear et al., 1996), and the conserved parts of the protein could be fitted onto the bacterial structure (Pear et al., 1996; Sethaphong et al., 2013), suggesting a conserved synthesis mechanism. Within the catalytic domain, two regions are plant specific (i.e. the plant-conserved region and the class-specific region; Pear et al., 1996; Vergara and Carpita, 2001). Genetic analysis, combined with coimmunoprecipitation experiments on detergent-solubilized membranes, show that higher plants have two types of CSC specialized for cellulose synthesis in primary and secondary cell walls (Kumar and Turner, 2014; McFarlane et al., 2014). Each of these CSC types contains three distinct CESA subunits. In Arabidopsis, this corresponds to CESA1, CESA3, and CESA6 for primary cell wall CSCs (Desprez et al., 2007; Persson et al., 2007) and CESA4, CESA7, and CESA8 for secondary wall CSCs (Taylor et al., 2003). Moreover, yeast split-ubiquitin interaction studies and in vivo bimolecular fluorescence complementation show that CESAs can form homodimers or heterodimers (Desprez et al., 2007; Timmers et al., 2009; Carroll et al., 2012). In addition to the CESAs, other proteins are associated at least with the primary cell wall CSC, such as the membrane-bound cellulase KORRIGAN1 (KOR1; Lei et al., 2014; Vain et al., 2014) and CELLULOSE SYNTHASE INTERACTING PROTEIN (CSI), which links CSCs to microtubules (Li et al., 2012). The exact stoichiometry of the CESAs within the CSC is not known. Such information is needed to understand the assembly of the CSC and the role of the different subunits in the formation of the crystalline microfibril. Here, we used coimmunoprecipitation and quantitative proteomics to determine the stoichiometry of the CESA subunits in primary cell wall CSCs.

[1] This work was supported by the European Union Framework Program 7 (project no. 211982; Renewall).

* Address correspondence to martine.gonneau@versailles.inra.fr.

The author responsible for distribution of materials integral to the findings presented in this article in accordance with the policy described in the Instructions for Authors (www.plantphysiol.org) is: Martine Gonneau (martine.gonneau@versailles.inra.fr).

[W] The online version of this article contains Web-only data.

www.plantphysiol.org/cgi/doi/10.1104/pp.114.250159

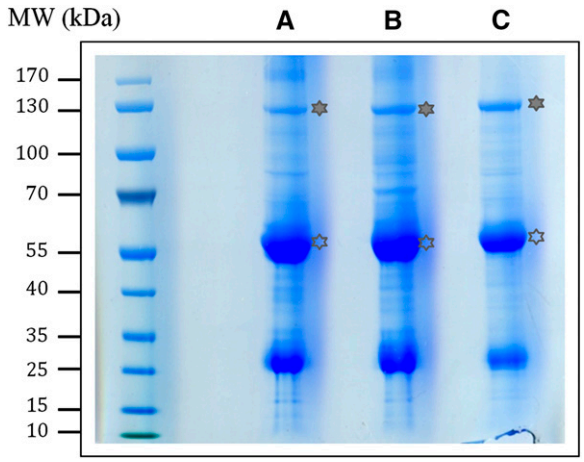

Figure 1. Coomassie Blue staining of proteins immunoprecipitated with specific primary CESA antibodies from *cesa2/cesa5* seedlings. Proteins were separated on NuPAGE 4% to 12% Bis-Tris gels/NuPAGE MOPS-SDS buffer. Lane A, Anti-CESA1; lane B, anti-CESA3; lane C, anti-CESA6. Gray stars indicate the positions of the bands used for mass spectrometry analysis, and unfilled stars indicate IgG.

RESULTS AND DISCUSSION

The Arabidopsis genome contains 10 CESA genes (Richmond and Somerville, 2000). In dark-grown seedlings, CSCs contain three CESAs: CESA1, CESA3, and a third class of CESAs, represented by CESA2, CESA5, CESA6, and CESA9 (collectively referred to as CESA6-like), which are thought to compete for the same position in the complex (Desprez et al., 2007; Persson et al., 2007). Finally, CESA10 is most closely related to CESA1, but its function has not been studied so far. To simplify the analysis of the stoichiometry of the CESA subunits in the CSC, we first removed the redundancy for CESA6 by using a *cesa2/cesa5* loss-of-function mutant. This double mutant has no visible phenotype as a dark-grown seedling or as an adult greenhouse-grown plant (Desprez et al., 2007). *CESA9* was not considered here, since it is primarily expressed in the seed coat and embryo with very low expression in young seedlings (Beeckman et al., 2002; Persson et al., 2007; Stork et al., 2010). We also did not study *CESA10*, since its transcript levels are highest in developing embryos and very low (at least 500-fold lower than *CESA1*) or undetectable in dark-grown seedlings (https://www.genevestigator.com/gv/). To reliably determine the stoichiometry of the three CESA isoforms in the CSC, we first immunoprecipitated the complex, using anti-CESA antiserum, prior to the liquid chromatography (LC)-tandem mass spectrometry (MS/MS) analysis. A problem with this approach is that the antiserum not only precipitates the protein complex but also free target CESA protein, which precludes any quantitative analysis of the stoichiometry in the complex. To circumvent this problem, we carried out three immunoprecipitations, using antisera against each of the three CESA isoforms, and only took into account in the analysis the respective nontarget proteins. In this way, we expected to quantify only the CESAs that were part of heteromeric protein complexes.

Total proteins were extracted from *cesa2/cesa5* young seedlings under nondenaturing conditions, and complexes were coimmunoprecipitated using three antibodies specifically directed against the N-terminal domain of CESA1, CESA3, and CESA6 (Desprez et al., 2007). The coimmunoprecipitation products were loaded on a denaturing one-dimensional electrophoresis gel. Each antibody precipitated a 120- to 130-kD band, a mass that corresponds to that of the CESA proteins (Fig. 1). These bands were extracted from the gel and processed for LC-MS/MS analysis. After in-gel tryptic digestion of the bands and LC-MS/MS analysis, we used label-free spectral counting to determine the relative abundance of the CESAs in the coimmunoprecipitated bands. The analysis of the LC-MS/MS data showed that, in each experiment, the total number of MS/MS spectra identified for the CESAs was comparable for the three coimmunoprecipitations (Table I). The sequence coverage for the three CESA proteins ranged from 25% to 35%, and the proteotypic peptides (a peptide sequence that is found only in one of the three CESAs) aligned all along the sequence of the proteins (Supplemental Table S1). As expected, the analysis showed that the coimmunoprecipitation resulted in the preferential enrichment of the isoform targeted by the antibody (Table I, in boldface). This also underscores the specificity of the three antibodies for the respective CESA isoforms. All the LC-MS/MS data (available in Supplemental Table S2) were analyzed using the X!Tandem open-source software (http://pappso.inra.fr/bioinfo/xtandempipeline/). We choose to express the relative abundance of the CESA using the protein abundance index (PAI). The PAI estimates the relative abundance of a protein and is calculated as the number of identified spectra divided by the number of theoretical peptides of the protein (theoretical peptide number corresponds to the number of peptides resulting from the theoretical digestion of the protein by trypsin and that are visible in mass spectrometry [i.e. having a mass ranging between 800 and 2500 D.]).

As mentioned above, for the pairwise ratios of the three CESAs calculated from the PAI, we only took into account the two nontarget isoforms for each coimmunoprecipitation. The relative ratios of the PAI values were as follows: CESA6:CESA3 = 1,062; CESA1:CESA6 = 1,009; and CESA3:CESA1 = 1,112 (Table II). Similar ratios were obtained when using the number of unique peptides or the number of specific peptides determined by

Table I. *Total number of spectra for each CESA isoform in the three coimmunoprecipitations*

Three technical repeats were used. Peptides of the targeted isoform are shown in boldface. coIP, Coimmunoprecipitation.

CESA	coIP-CESA1	coIP-CESA3	coIP-CESA6
CESA1	**22-11-14**	14-9-6	11-5-12
CESA3	9-7-9	**24-22-15**	21-7-11
CESA6	11-6-10	11-11-7	**38-13-22**
Total no. of spectra	99	119	140

Table II. *The PAI is the ratio between the total number of spectra obtained during the protein identification process on the theoretical number of peptides ranging between 800 to 2,500 D and detectable by mass spectrometry for a given protein*

Three technical repetitions were performed for each coimmunoprecipitation (three LC-MS/MS analyses of the peptides extracted from each 120-kD band [X!Tandem pipeline parser 3.2]). IP, Immunoprecipitation. Italic entries represent the ratio of the PAI of the IP-targeted isoform on the PAI of the less represented isoform.

CESA	Coverage	Mass	PAI											
			Anti-CESA1				Anti-CESA3				Anti-CESA6			
			IP1-1	IP1-2	IP1-3	Mean	Ratio	IP3-1	IP3-2	IP3-3	Mean	Ratio	IP6-1	IP6-2	IP6-3	Mean	Ratio
	%	*kD*															
CESA1	25	122.0	0.610	0.317	0.366	0.431	*1.872*	0.439	0.220	0.171	0.276	1.009	0.366	0.220	0.293	0.293	1.000
CESA3	38	119.5	0.262	0.190	0.238	0.230	1.000	0.667	0.667	0.452	0.595	*2.172*	0.500	0.190	0.286	0.325	1.112
CESA6	30	122.3	0.289	0.178	0.267	0.244	1.062	0.333	0.289	0.200	0.274	1.000	1.000	0.378	0.578	0.652	*2.227*

X!Tandem (see green boxes in Supplemental Table S2). In conclusion, our results support a 1:1:1 stoichiometry of CESA1, CESA3, and CESA6 in the primary cell wall CSC.

Our results exclude previous models based upon a 1:2:3 ratio of CESA isoforms in the complex (Ding and Himmel, 2006), but they do not allow the distinction between models based on three or six subunits per globule: that is to say, 18 (3 × 6) or 36 (6 × 6) CESAs per CSC. If we assume that each CSC produces one elementary microfibril and that all CESAs in the CSC are catalytically active, this would correspond to either 18 or 36 glucan chains per microfibril. Most spectroscopic and diffraction techniques converge on a diameter of around 3 nm for an elementary microfibril, which is too small to contain 36 chains. In addition, a recent study (Newman et al., 2013) showed that best fits with x-ray diffraction data are obtained either with models based on 18 glucan chains, when allowing for occasional coalescence (or twinning) between microfibrils, or 24 chains, without twinning.

The latter 24-chain model would imply that each CSC globule contains four CESAs, a possibility that can be excluded given the 1:1:1 stoichiometry of the three CESAs and if one assumes that all CESAs in the complex are active. A model with 6 × 3 CESAs, therefore, would best fit the microfibril structural data; however, it would contradict observations suggesting CESA dimerization (Kurek et al., 2002; Olek et al., 2014) or the presence of even-numbered oligomers (dimers and tetramers) and no trimers in coimmunoprecipitation experiments on secondary cell wall CSCs (Atanassov et al., 2009).

Our proteomic analysis was carried out on a *cesa2/cesa5* double mutant, in which CESA6 is expected to act nonredundantly (the fourth CESA6-like isoform, CESA9, is not expressed in dark-grown seedlings). However, in wild-type plants, CESA2 and CESA5 compete for the same position in the complex, suggesting the presence of distinct CSC subpopulations. Therefore, it will be interesting to study the stoichiometry of CSCs also in a wild-type context. Finally, it will be important to determine also the stoichiometry of other proteins, such as KOR1 or CSI, within the CSC.

MATERIALS AND METHODS

Plant Material and in Vitro Growth Conditions

Arabidopsis (*Arabidopsis thaliana*) wild-type ecotype Columbia-0 and *cesa2/cesa5* double mutant lines (Desprez et al., 2007) in the Columbia-0 background were grown in the dark at 20°C without Suc as described (Desprez et al., 2007).

Coimmunoprecipitation Experiments

Thirty grams of 3-d-old dark-grown *cesa2/cesa5* seedlings was ground in liquid nitrogen, and the powder was transferred to either 6 mL of immunoprecipitation buffer (50 mM Tris-HCl, pH 8, 150 mM NaCl, and 2% [v/v] Triton X-100, containing 1% [w/v] insoluble polyvinylpyrrolidone [Polyclar AT], plant protease inhibitor cocktail, and phosphatase inhibitor mixtures 2 and 3 [Sigma] used, respectively, at 100- and 200-fold dilutions). A cleared cell lysate was obtained by centrifugation at 8,000*g* for 10 min and filtration of the supernatant through Miracloth. The supernatant

was split into three equal fractions and supplemented with the purified polyclonal antisera directed against CESA1, CESA3, and CESA6 at 1:400, 1:50, and 1:200 respectively. The immunoprecipitations were carried out according to established protocols (Harlow and Lane, 1999). CESA proteins bound on Protein A-Dynabeads were heated for 10 min at 80°C in Laemmli buffer, and SDS-PAGE was performed using NuPAGE 4% to 12% Bis-Tris 10-well gels with NuPAGE MOPS-SDS running buffer.

Sample Preparation and in-Gel Digestion

After GelCode Blue staining (Thermo Scientific) of the SDS-PAGE gel, the bands corresponding to the CESA expected mean size (120 kD) were taken from the three immunoprecipitation lanes and cut into 1- to 2-mm^3 pieces. Gel pieces were washed twice with 50 mM NH_4HCO_3 and 50% (v/v) CH_3CN, dried at room temperature, and digested overnight at 37°C with 100 ng of sequencing-grade modified trypsin (Promega) in 50 mM NH_4HCO_3. The supernatant of trypsin hydrolysis was transferred to a new tube, and the gel slices were extracted (1) with 25 μL of 50 mM NH_4HCO_3 and (2) two times with 25 μL of 0.1% (v/v) HCOOH and 50% (v/v) CH_3CN. For each extraction, the gel slices were incubated for 15 min at room temperature while shaking. The supernatants of each extraction were pooled with the original trypsin digest supernatant and dried for 1 h in a SpeedVac concentrator. The peptides were then solubilized in 0.08% (v/v) trifluoroacetic acid in 2% (v/v) acetonitrile prior to LC-MS/MS analysis.

LC-MS/MS Identification and Quantification of the Copurified Proteins

LC-MS/MS analysis was performed on an Ultimate 3000 LC system (Dionex) connected to an LTQ Orbitrap Discovery mass spectrometer (Thermo Fisher) with a nanoelectrospray ion source to realize the separation, ionization, and fragmentation of peptides, respectively. The raw data produced on the LTQ Orbitrap mass spectrometer were first converted into mzXML files with ReADW (http://proteomecenter.org). Protein identification was performed with X!Tandem software (X!Tandem tornado 2008.02.01.3; http://www.thegpm.org) against a protein database of Arabidopsis (The Arabidopsis Information Resource 7) as well as a proteomic contaminant database (for details of the parameters used, see Supplemental Table S2).

Label-Free Method for the Relative Quantification of the CESA Isoforms Using LC-MS/MS Data

For relative quantification of the CESA isoforms, we used the number of spectra obtained during protein identification by mass spectrometry. The number of spectra is admitted to be proportional to the abundance of a given protein. For each CESA, we calculated an abundance factor derived from the PAI developed by Ishihama et al. (2005). The experimental number of spectra was normalized according to the theoretical number of peptides released after trypsin hydrolysis and having a mass ranging between 800 and 2,500 D. Therefore, the abundance index represents the relative abundance of a given protein taking into account its mass and tryptic digestibility.

Supplemental Data

The following materials are available in the online version of this article.

Supplemental Table S1. Proteotypic peptides.

Supplemental Table S2. Proteomic raw data.

Received September 22, 2014; accepted October 25, 2014; published October 28, 2014.

LITERATURE CITED

Atanassov II, Pittman JK, Turner SR (2009) Elucidating the mechanisms of assembly and subunit interaction of the cellulose synthase complex of Arabidopsis secondary cell walls. J Biol Chem **284:** 3833–3841

Beeckman T, Przemeck GK, Stamatiou G, Lau R, Terryn N, De Rycke R, Inzé D, Berleth T (2002) Genetic complexity of cellulose synthase A gene function in Arabidopsis embryogenesis. Plant Physiol **130:** 1883–1893

Brown RM, Saxena IM (2007). Cellulose: Molecular and Structural Biology Dordrecht. Springer, Dordrecht, The Netherlands

Carroll A, Mansoori N, Li S, Lei L, Vernhettes S, Visser RG, Somerville C, Gu Y, Trindade LM (2012) Complexes with mixed primary and secondary cellulose synthases are functional in Arabidopsis plants. Plant Physiol **160:** 726–737

Desprez T, Juraniec M, Crowell EF, Jouy H, Pochylova Z, Parcy F, Höfte H, Gonneau M, Vernhettes S (2007) Organization of cellulose synthase complexes involved in primary cell wall synthesis in Arabidopsis thaliana. Proc Natl Acad Sci USA **104:** 15572–15577

Ding SY, Himmel ME (2006) The maize primary cell wall microfibril: a new model derived from direct visualization. J Agric Food Chem **54:** 597–606

Harlow E, Lane DR (1999). Using Antibodies: A Laboratory Manual. Cold Spring Harbor Laboratory Press, Cold Spring Harbor, NY

Harris D, Bulone V, Ding SY, DeBolt S (2010) Tools for cellulose analysis in plant cell walls. Plant Physiol **153:** 420–426

Ishihama Y, Oda Y, Tabata T, Sato T, Nagasu T, Rappsilber J, Mann M (2005) Exponentially modified protein abundance index (emPAI) for estimation of absolute protein amount in proteomics by the number of sequenced peptides per protein. Mol Cell Proteomics **4:** 1265–1272

Kumar M, Turner S (2014) Plant cellulose synthesis: CESA proteins crossing kingdoms. Phytochemistry (in press) 10.1016/j.phytochem.2014.07.009

Kurek I, Kawagoe Y, Jacob-Wilk D, Doblin M, Delmer D (2002) Dimerization of cotton fiber cellulose synthase catalytic subunits occurs via oxidation of the zinc-binding domains. Proc Natl Acad Sci USA **99:** 11109–11114

Lei L, Zhang T, Strasser R, Lee CM, Gonneau M, Mach L, Vernhettes S, Kim SH, Cosgrove JD, Li S, et al (2014) The *jiaoyao1* mutant is an allele of *korrigan1* that abolishes endoglucanase activity and affects the organization of both cellulose microfibrils and microtubules in *Arabidopsis*. Plant Cell **26:** 2601–2616

Li S, Lei L, Somerville CR, Gu Y (2012) Cellulose synthase interactive protein 1 (CSI1) links microtubules and cellulose synthase complexes. Proc Natl Acad Sci USA **109:** 185–190

McFarlane HE, Döring A, Persson S (2014) The cell biology of cellulose synthesis. Annu Rev Plant Biol **65:** 69–94

Morgan JL, Strumillo J, Zimmer J (2013) Crystallographic snapshot of cellulose synthesis and membrane translocation. Nature **493:** 181–186

Newman RH, Hill SJ, Harris PJ (2013) Wide-angle x-ray scattering and solid-state nuclear magnetic resonance data combined to test models for cellulose microfibrils in mung bean cell walls. Plant Physiol **163:** 1558–1567

Olek AT, Rayon C, Makowski L, Kim HR, Ciesielski P, Badger J, Paul LN, Ghosh S, Kihara D, Crowley M, et al (2014) The structure of the catalytic domain of a plant cellulose synthase and its assembly into dimers. Plant Cell **26:** 2996–3009

Pear JR, Kawagoe Y, Schreckengost WE, Delmer DP, Stalker DM (1996) Higher plants contain homologs of the bacterial celA genes encoding the catalytic subunit of cellulose synthase. Proc Natl Acad Sci USA **93:** 12637–12642

Persson S, Paredez A, Carroll A, Palsdottir H, Doblin M, Poindexter P, Khitrov N, Auer M, Somerville CR (2007) Genetic evidence for three unique components in primary cell-wall cellulose synthase complexes in Arabidopsis. Proc Natl Acad Sci USA **104:** 15566–15571

Richmond TA, Somerville CR (2000) The cellulose synthase superfamily. Plant Physiol **124:** 495–498

Sethaphong L, Haigler CH, Kubicki JD, Zimmer J, Bonetta D, DeBolt S, Yingling YG (2013) Tertiary model of a plant cellulose synthase. Proc Natl Acad Sci USA **110:** 7512–7517

Stork J, Harris D, Griffiths J, Williams B, Beisson F, Li-Beisson Y, Mendu V, Haughn G, Debolt S (2010) CELLULOSE SYNTHASE9 serves a nonredundant role in secondary cell wall synthesis in Arabidopsis epidermal testa cells. Plant Physiol **153:** 580–589

Taylor NG, Howells RM, Huttly AK, Vickers K, Turner SR (2003) Interactions among three distinct CesA proteins essential for cellulose synthesis. Proc Natl Acad Sci USA **100:** 1450–1455

Timmers J, Vernhettes S, Desprez T, Vincken JP, Visser RG, Trindade LM (2009) Interactions between membrane-bound cellulose synthases involved in the synthesis of the secondary cell wall. FEBS Lett **583:** 978–982

Tsekos I (1999) The sites of cellulose synthesis in algae: diversity and evolution of cellulose-synthesizing enzyme complexes. J Phycol **35:** 635–655

Vain T, Crowell EF, Timpano H, Biot E, Desprez T, Mansoori N, Trindade LM, Pagant S, Robert S, Höfte H, et al (2014) The cellulase KORRIGAN is part of the cellulose synthase complex. Plant Physiol **165:** 1521–1532

Vergara CE, Carpita NC (2001) Beta-D-glycan synthases and the CesA gene family: lessons to be learned from the mixed-linkage (1→3),(1→4)beta-D-glucan synthase. Plant Mol Biol **47:** 145–160